

LIQUID DISTRIBUTION BEHAVIOUR OF CONVENTIONAL AND HIGH CAPACITY STRUCTURED PACKINGS

Ž. Olujić,* R. van Baak, J. Haaring
Delft University of Technology, Delft, The Netherlands

Large scale air/water experiments have been carried out to observe the effects of variation in influential parameters on liquid distribution behavior of a high capacity corrugated sheet structured packing (Montz Pak B1-250M) and to compare it with that of its conventional counterpart (Montz Pak B1-250). The liquid distribution performance of both packings appeared to be consistently good and, surprisingly, the high capacity version outperformed in the quality the conventional packing, but at the expense of a more pronounced wall flow, which however appeared to be less sensitive to high gas loads.

KEYWORDS: distillation, structured packing, liquid distribution, maldistribution

INTRODUCTION

It is well known that achieving a good quality of liquid distribution is crucial for performance of corrugated sheet structured packings [1–3]. By practical experiences and the research work done in late 1980s and beginning 1990s, the sources and the nature of large scale liquid maldistribution have been revealed [4–9]. The often insufficient quality of initial distribution appeared to be a major wrongdoer and since then the high performance liquid distributors are preferred to ensure utilizing the full potential of a structured packing as a vapor/liquid contacting device.

Nowadays, high capacity packings (Montz-pak M, Mellapak Plus and Flexipac HC series) are getting more and more attention [10], because this new generation structured packings allow revamping the columns equipped with conventional packings. A key feature of these packings is a significantly lower pressure drop, which was achieved by avoiding the sharp vapor flow direction changes at the transitions between packing elements. This occurred simply by bending the bottom part of corrugations to vertical. This alone or in combination with similar bends in upper part of corrugations creates a smoother transition for both phases, i.e. shifts the build-up of liquid to higher vapor loads and consequently enables operation with a significantly higher capacity than that achieved with the conventional counterparts of the same size. This has been proven in both hydraulic and total reflux tests [10–12].

Interestingly, the total reflux experiments carried out with high capacity Montz packings, characterized by a rather long bend in the bottom part of corrugations (see Figure 1), indicated a certain loss of efficiency in the preloading region [12]. Since the vapor is practically not affecting the liquid distribution in the preloading region, new

*Correspondence author: Dr. Ž. Olujić, Laboratory for process equipment, Delft University of Technology, Leegwaterstraat 44, 2628 CA Delft, The Netherlands. E-mail: z.olujic@3me.tudelft.nl

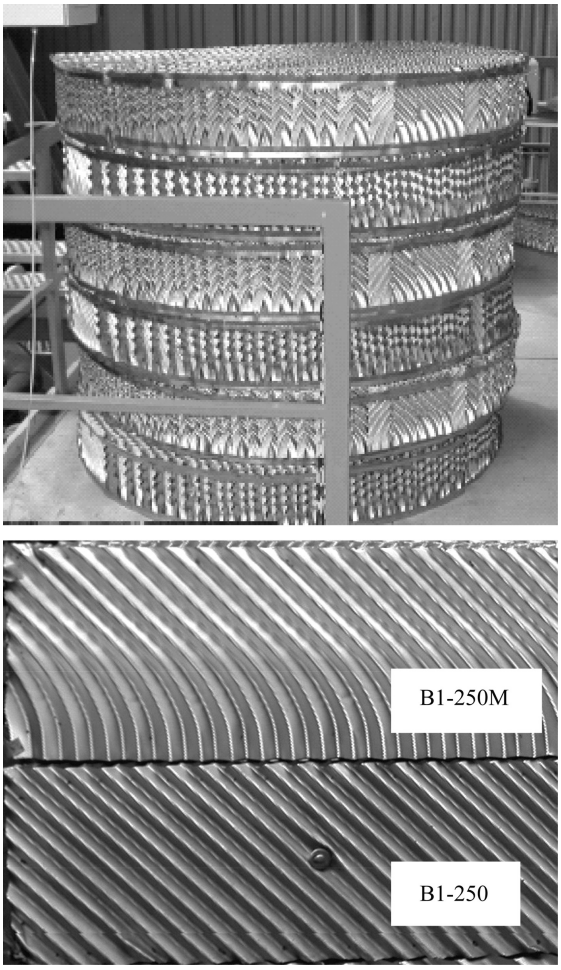

Figure 1. A bed of B1-250M (above) and corrugated sheets of B1-250M and B1-250

flow channel geometry has been indicated as a possible source of certain deterioration in liquid distribution. In order to provide an answer to this question, an experimental study was arranged using large diameter, column hydraulics simulator available at the Delft University of Technology.

The objective of this paper is to present experimental evidence on the liquid distribution behavior of B1-250M and to compare it with that of its conventional counterpart, Montz-pak B-250, which is the reference packing evaluated in various ways in numerous studies. As it will be shown in what follows, B1-250M proved to posses superb liquid distribution properties.

EXPERIMENTAL STUDIES

PACKINGS TESTED

Figure 1 shows photographs of a bed of B1-250M packing and the corrugated sheets of B1-250M and B1-250, indicating the main difference in the geometry of the flow channels. The size of these well known, unperforated shallow embossed packings is 250 m^2/m^3. Packing element height of B1-250 is approximately 0.2 m and that of B1-250M few millimeters larger. Each packing layer was assembled of three packing segments and the packing layers were stacked to form a bed of desired height. According to the common practice, each subsequent layer was rotated by 90^0 to the previous one.

EXPERIMENTAL SETUP

The necessary experiments were performed using the large diameter column hydraulics' simulator available at the Delft University of Technology. Figure 2 shows a 3-D drawing of this installation. The hart of the experimental set-up is a 1.4 m ID column consisting of a number of flanged Plexiglas sections, which allows installation of beds with heights up to 6 m. The transparent part of the column is supported by stainless steel column sump, which is made broader (1.8 m ID) to accommodate gas inlet distributor, which distributed air delivered by a powerful, electronically controlled blower (capacity, up to 8 m^3/s). Water from the supply tank was pumped through the pipes containing a magnetic flow meter by a centrifugal pump (110 m^3/h) to the top of the column, at an elevation of approximately 10 m.

Liquid was distributed using a narrow trough distributor containing 152 drip tubes which is an equivalent to 100 drip points per meter square. The essential piece of equipment used in this study was the liquid collecting system, shown in Figure 3. Liquid distribution measurements were conducted using a flanged short column segment containing three equidistantly placed moving rods, each with a movable funnel (50 mm × 50 mm) at the end. The rectangular funnels were equipped with electrodes at different heights to indicate the level of liquid in the funnel by switching on the corresponding lamp. At low level position the stopwatch went on and the time was stopped after reaching the upper level. In other words, the whole measurement work has been performed relying on the reliable, but work intensive time-volume technique. Namely, for each situation the same procedure was repeated for 25 locations (50 mm spacing) along each of three cross sectional directions. Fortunately, the reproducibility of measurements proved to be high. Tap water was used at ambient conditions, and only in a limited number of cases the liquid distribution was measured in the presence of a counter currently

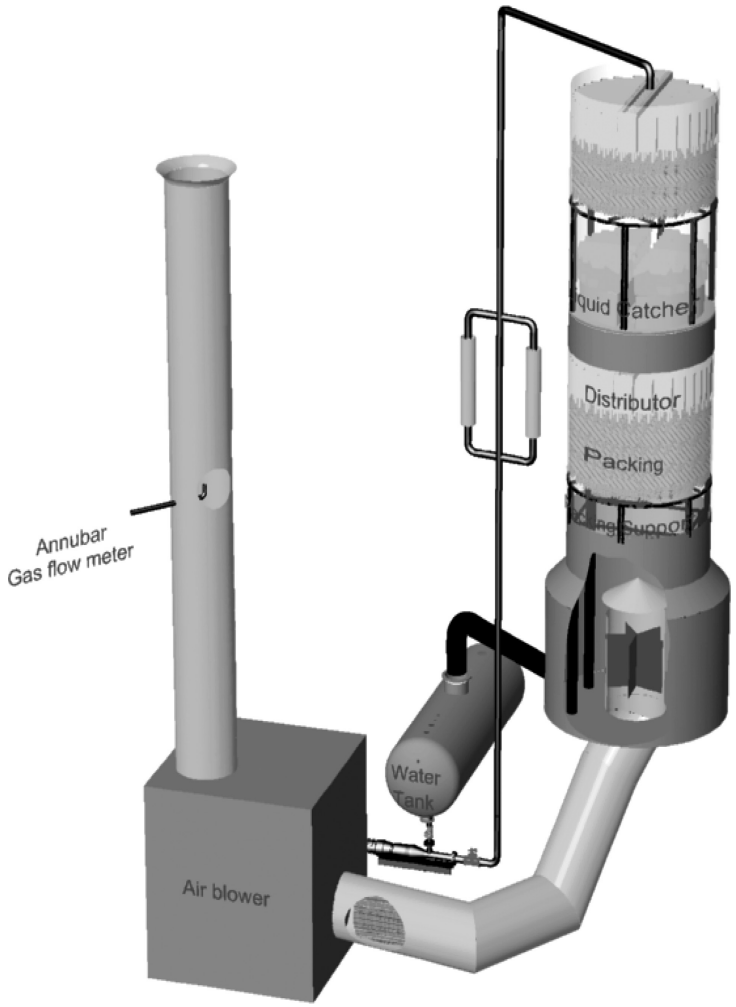

Figure 2. 3D image of the TU Delft column hydraulics' simulator

flowing air stream. Although the funnel design was highly aerodynamic, liquid collecting at high gas loads occurred with difficulties.

A unique feature of the liquid collecting setup is the double wall arrangement (narrow annulus at the periphery) which allows collection of the liquid leaving the bed section via column walls.

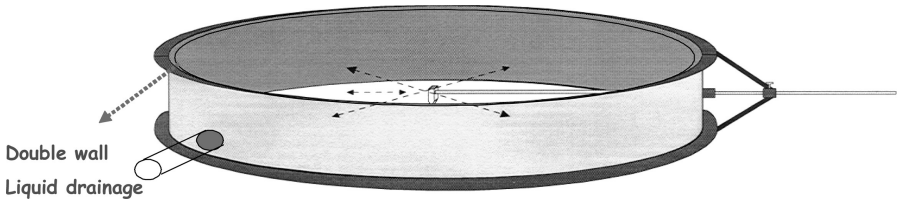

Figure 3. Schematic of the liquid collection section containing six equidistantly placed liquid drainage pipes

Finally, the pressure drop over the bed was measured for each test configuration using a fine pressure drop cell integrated into a state of the art digital device.

DATA PRESENTATION

As indicated in Figure 3, the liquid samples from the bulk flow were collected along three equidistantly arranged directions, with a collection resolution corresponding to the dimensions of the funnel (50 mm × 50 mm). This grid size gave a detailed enough indication of the liquid distribution along three sampling directions. The measured velocity profiles are shown on the left hand side of the Figure 4, as a fluctuating line compared to corresponding horizontal line representing average (superficial) velocity. The numbers below each of these three plots indicate the direction of sampling according to the situation shown in

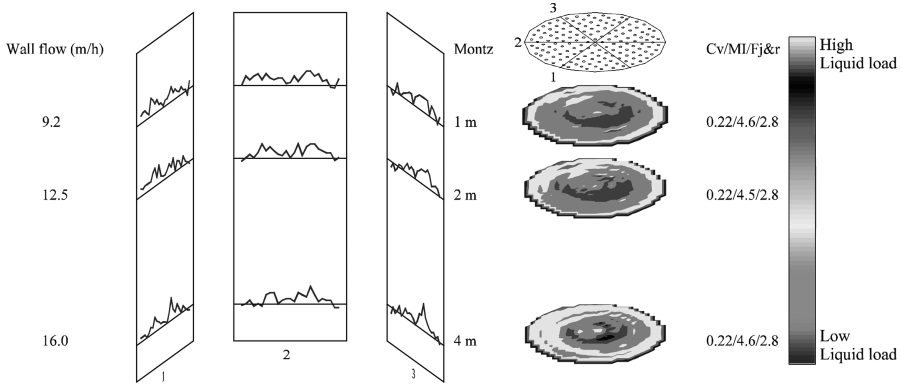

Figure 4. Effect of the packed bed height on the liquid distribution quality of B1-250 at a liquid load of 10 m^3/m^2h, without gas flow. From left to the right: wall flow extent, profiles measured along three liquid collection directions, interpolated 2D full cross sectional profiles, the corresponding maldistribution indicators and the liquid loads associated with 2D full cross section profiles

the next column representing full cross sectional profiles with the layout of the drip points on the top. These 2D liquid distribution profiles were obtained by linear interpolation of measured values belonging to the same concentric circle (12 in total). This approximation provided an idea on the extent of clustering in local velocities, as well as a visual impression on the flow distribution pattern, represented by colored cross section slices, which are reproduced here in black-white. The vertical bar on the right hand side indicates the corresponding liquid loads by a distinctive color; however the black-white version shown here is not clear enough in this respect. In addition, the column on the left hand end indicates the amount of wall flow expressed as the liquid load, i.e. superficial liquid velocity in meters per hour. The corresponding numbers were obtained by dividing the volumetric flow rate of collected wall flow by the cross sectional area fraction occupied by the annulus.

These plots, i.e. corresponding numbers provide a basis for the evaluation of the quality of cross sectional liquid distribution using standard, one-dimensional liquid (mal)distribution characterization means, such as the well-known maldistribution factor, i.e. the coefficient of variation of the velocity measurements.

LIQUID MALDISTRIBUTION CHARACTERIZATION

For a column cross section with a grid superimposed, the coefficient of variation, C_v, is defined as

$$C_v = \left[\frac{1}{A_t}\sum_{i=1}^{N} A_i\left(\frac{u_i - \overline{u}}{\overline{u}}\right)^2\right]^{0.5} \tag{1}$$

where A_t is the total cross sectional area, A_i is the area of a cell, u_i is local, grid cell velocity, and N is the total number of cells. The overall mean velocity is defined as

$$\overline{u} = \frac{1}{A_t}\sum_{i=1}^{N} A_i u_i \tag{2}$$

A C_v approaching zero indicates a uniform (plug) flow situation. However C_v, which is an absolute measure for the magnitude of maldistribution, does not give any idea about cross sectional distribution of flow variations, i.e. the nature of the maldistribution, Billingham and Lockett [13] introduced a new coefficient *Cm* that distinguishes between small- and large-scale forms of maldistribution. *Cm* is evaluated in an identical manner as the coefficient of variation, C_v, except a local mean velocity rather than an overall mean velocity is used in its calculation. The corresponding expression is

$$Cm = \left[\frac{1}{A_t}\sum_{i=1}^{N} A_i\left(\frac{u_i - \overline{u_i}}{\overline{u_i}}\right)^2\right]^{0.5} \tag{3}$$

where $\overline{u}_i$ is the local mean velocity associated with cell i, calculated by

$$\overline{u_i} = \frac{\sum \delta_{ij}(A_i u_i + A_j u_j)}{\sum \delta_{ij}(A_i + A_j)} \tag{4}$$

where $\delta_{ij} = 1$, if i and j are neighbors, and $\delta_{ij} = 0$, if i equals j or the cells do not share a common border. Detailed information on the use of equation (4) can be found in the original paper [13]. In essence, this approach allows for the effect of clustering the flow variations, depending on the grid size.

The ratio of C_v and Cm is defined as the maldistribution index:

$$MI = \frac{C_v}{Cm} \tag{5}$$

Being related to *Cm, MI* also depends on the grid size. If the flow variations are clustered into large groups Cm is much less than C_v, and this leads to a large *MI*, i.e. to a large scale maldistribution. However, if accompanying C_v is low than a large *MI* is not so harmful. In other words, the coefficient of variation, C_v, is still indispensable as the measure of the difference in the magnitude of maldistribution. As experienced while evaluating the present data, it become obvious that MI does not improve when the profile is getting more uniform, because C_m appeared to decrease much faster than C_v.

Certainly, both C_v and C_m are well defined parameters, however it appeared difficult to derive an analytical relation which would represent more closely the physical picture. Therefore an empirical solution was chosen, considering four extremes in the values of two maldistribution factors, i.e. large C_v in conjunction with a small and a large C_m and small C_v in conjunction with a small and a large C_m, respectively. In present case, the C_v varies between 0 and 1, and C_m between 0.035 and 0.1. The values that go beyond upper limits are extreme regarding the extent of maldistribution involved.

New dimensionless empirical maldistribution index, $F_{J\&R}$, is shown as a 3D plot in Figure 5. Values below 2 indicate a good distribution (C_v below 0.2), values between 2 and 4 (C_v values below 0.3) a moderate maldistribution and larger values a severe maldistribution. In essence, new maldistribution indicator (index) is made practically insensitive to the grid size and follows C_v in trend. In this way it represents a more appropriate indication of the extent of large scale maldistribution associated with the hydraulic operation of a packed bed. As illustrated in Figure 4, all data sets contain corresponding C_v, *MI* and $F_{J\&R}$ numbers.

RESULTS AND DISCUSSION

Figure 6 shows the effect of the gas load on the distribution quality at a packed depth of 1 m, for B1-250M packing operating with a constant liquid load of 10 m^3/m^2h (m/h).

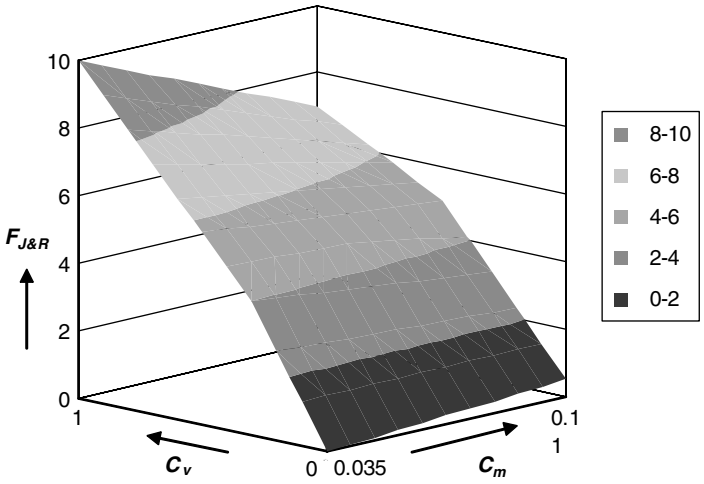

Figure 5. New empirical maldistribution indicator

Four slices/profiles show situations, from top to bottom, corresponding to the operation without gas, with a counter current gas flow around loading point (F-factor = 2.11 $Pa^{0.5}$), in the loading region (F-factor = 2.78 $Pa^{0.5}$) and under flooding conditions (F-factor = 3.68 $Pa^{0.5}$), respectively. On the left hand side, we can see that the wall flow tends to decrease with increasing gas load. At the largest F-factor packing, close to

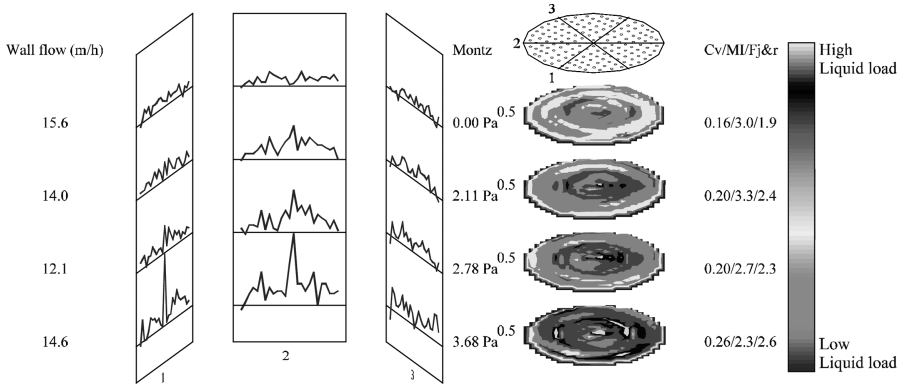

Figure 6. Effect of the gas load on liquid distribution of 1 m bed of B1-250M, at a liquid load of 10 m^3/m^2h

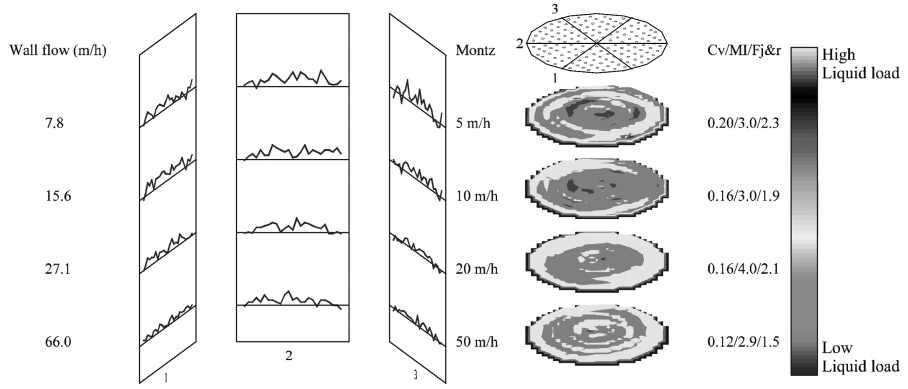

Figure 7. Effect of the liquid load on liquid distribution quality of 1 m bed of B1-250M

the flooding point, this packing still operates quite smoothly, with some tendency to accumulate the liquid in the centre of the bed. In general, the quality of liquid distribution under normal operating conditions is similar to that obtained without presence of gas flow. Therefore, most of the tests have been carried out without the countercurrent flow of gas.

Figure 7 shows the effect of the liquid load. As expected, the amount of wall flow increases with increasing liquid load and relatively more liquid is contained in the wall zone than in the bulk. However, as mentioned above, this is not so pronounced in the presence of the ascending gas flow, which effectively prevents liquid from accumulating in the wall zone. In general, with increasing liquid load the quality of the distribution in the bulk of packing increases and from both visual observations and corresponding maldistribution indicators it can be concluded that this packing is very good in this respect. As illustrated in Figure 8, which compares this packing with its conventional counterpart, B1-250, taking the effect of packed height into consideration, the high capacity packings performs even better. This surprising result is clearly illustrated in the Figure 9 which shows corresponding C_v, MI and $F_{J\&R}$ maldistribution indicators as a function of the liquid load. It should be noted that observed profiles with velocity fluctuations around 20% represent in fact that what is generally called the natural distribution pattern for this kind of packings. This is well above say 10% for flow from drip tubes/points that is considered as upper limit for a good quality of initial distribution [14]. New standards have been formulated appropriately by Moore and Rukovena [15] and the irrigation accuracy of modern high performance narrow trough distributors is below 5% deviation in the individual flows.

Other results of this comprehensive study, which will be documented in another paper addressing the relation between the quality of the initial distribution and the bed performance, indicate clearly that in the practice it is more important to have a uniform distribution of drip tubes/points than a so uniform accuracy of drip points. In any case,

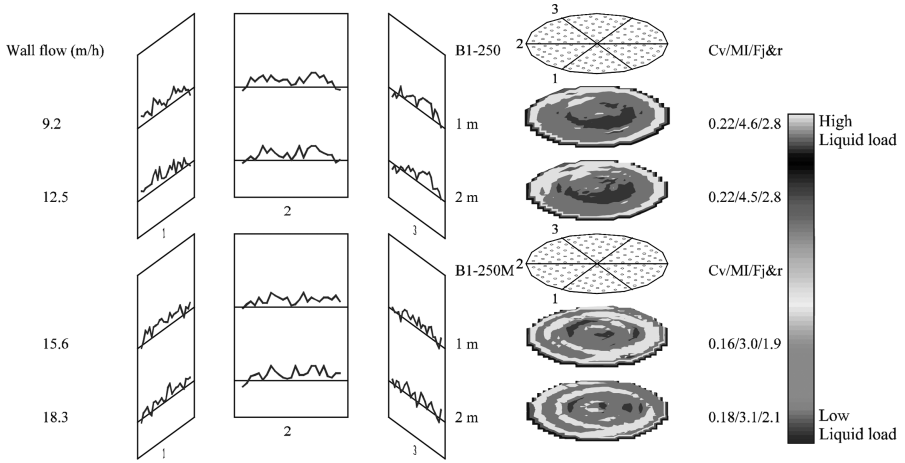

Figure 8. Effect of the packed height on liquid distribution quality of 1 m beds of B1-250 and B1-250M

for packing size studied, better distribution quality is not possible, i.e. observed profiles can be considered as the best real life approach to the plug flow.

A closer look at the plots in Figure 9 indicates that new maldistribution indicator follows the trend of C_v, and thus provides a more realistic picture of the degree of the liquid maldistribution associated with the observed flow patterns.

Figure 10 shows corresponding wall flow factors (ratio of measured wall zone load and the average liquid load) as a function of respectively the liquid load and the gas load.

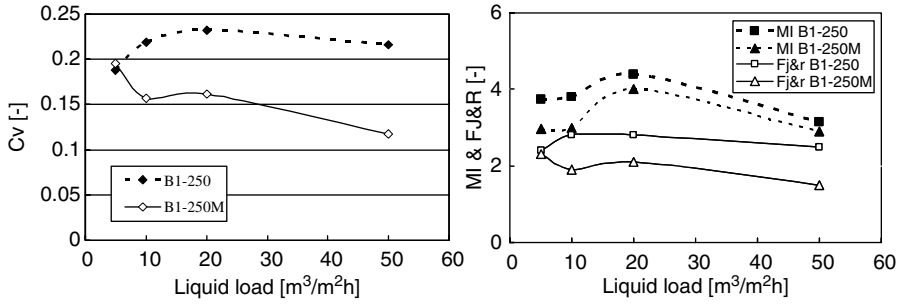

Figure 9. Liquid mal distribution indicators for B1-250 and B1-250M as a function of the liquid load

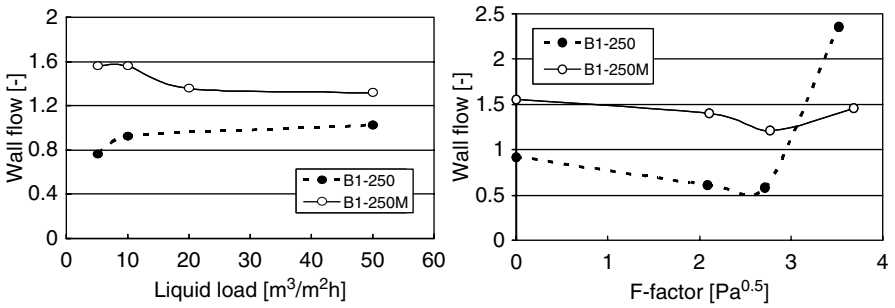

Figure 10. Effect of the liquid load (left) and the gas load (right, liquid load = 10 m^3/m^2h) on the extent of wall flow of B1-250 and B1-250M (bed height 1 m)

Obviously the wall flow of B1-250M packing is more pronounced. This may be attributed to two combining effects, i.e. the tendency to bring more liquid to the wall and to a reduced capacity regarding the ability to bring the liquid scrapped from the wall back into the bed. In fact, both packings use the same type of wall scrappers and in this respect similar performance should be expected.

However the different flow channels geometry influences directly the extent of the lateral spreading of these packings. This became obvious from a simple point source distribution experiment carried out with two sheets of each packing. Figure 11 shows the result. It should be noted that the liquid was introduced on the sheet with the channels oriented to the right, which implies that the liquid entering at location 7 and following this channel should leave it at the position 13. However, we find the liquid in nearly all channels, also on the opposite side. This means that the liquid spreading into a film tends also to follow gravity and flows at steeper angle than that of the corrugation. In other words, it tends to flow over the corrugation ridges and at the points where corrugation ridges of oppositely oriented channels touch each other a portion of the liquid is transferred to the channels of the neighboring sheet oriented to the left. As known from previous similar experiments [7] this local, liquid distributing crossings point mechanism is a characteristics of B1-250. Other packings show a more pronounced channel flow, which is also the case with B1-250M to some extent. Namely, though made from the same material this packing has got a shorter corrugation base, i.e. a narrower channel in the upper, inclined part, which discourages the liquid to flow over the corrugation ridges and consequently reaching the crossing points. Therefore more of the introduced liquid is transported to the side, i.e. the extent of lateral transport within one packing layer is larger. This may mean that in the wall zone relatively more liquid is brought onto the wall. On the other hand, with rather long bends the liquid scrapped from the wall which enters the channels in the lower half of the element height is not transported deeper into the bed but remains close to the wall. This seems to be a plausible explanation

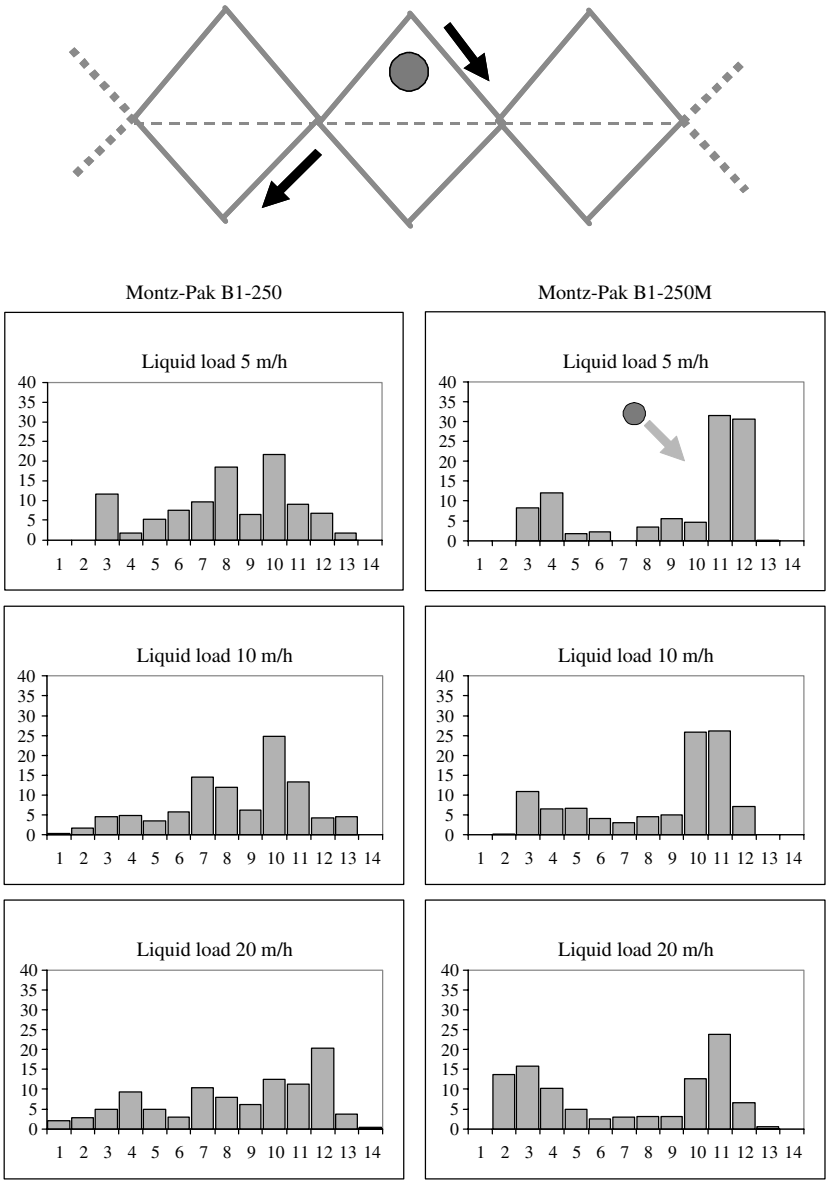

Figure 11. Point source liquid spreading characteristics of B1-250 and B1-250M at different liquid loads

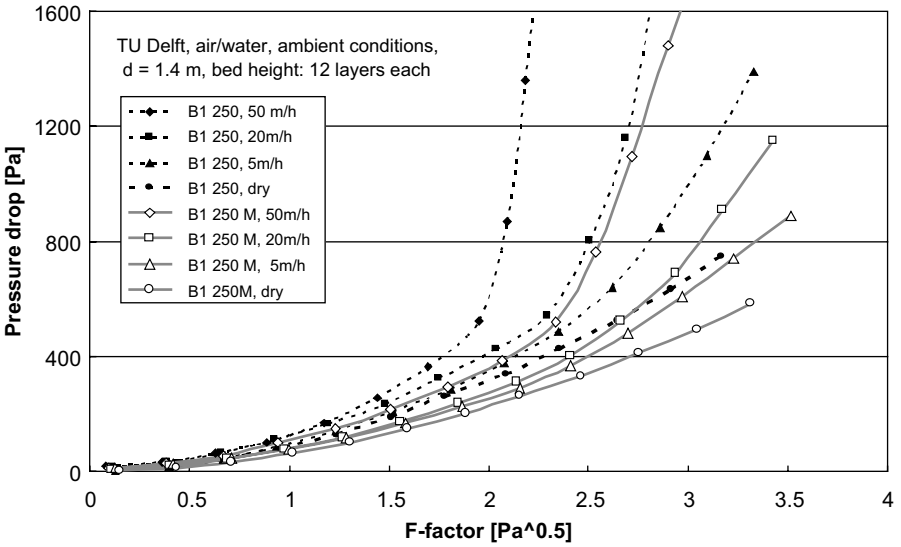

Figure 12. Measured pressure drop of B1-250 and B1-250M beds comprising 12 packing layers each, at different liquid loads

for the observed increased liquid load in the wall zone, which, as it can be seen from Figure 6, remains practically unaffected by the gas load even in the loading region.

The relative difference in pressure drop and consequently the capacity of B1-250 and B1-250M can be conjectured for from Figure 12. The measured pressure drop is shown here for the whole bed height involved (each bed consisting of 12 layers of packing) as a function of gas load for a number of liquid loads. This indicates that a significant capacity gain can be expected if B1-250 is replaced by B1-250M in an existing column.

CONCLUSIONS

Liquid distribution performances of conventional (B1-250) and high capacity (B1-250M) structured packings were measured and compared. Liquid distribution is practically not affected by gas flow in preloading region. Natural distribution quality (expressed via C_v) of B1-250 around 22% and of B1-250M around 15%, indicating a smoother performance of B1-250M.

A new empirical maldistribution indicator, $F_{J\&R}$, is introduced which combines both the magnitude (C_v) and the nature of maldistribution (C_m) in a realistic way. Expressed in numbers, a liquid distribution pattern with a $F_{J\&R}$ value below 3 may be considered practically as maldistribution free.

In case of B1-250 the wall flow increases with both the liquid load and bed depth, however never exceeding 4% of total flow. The gas flow prevents excessive accumulation of the liquid in the wall zone. The wall flow of B1-250M it is somewhat larger and practically independent of gas flow, also in the loading region. The more pronounced lateral spreading of B1-250M is responsible for bringing more liquid to the wall and a rather long bend for a limited transport of the liquid from the wall into the bulk of the packing.

Pressure drop of B1-250M is significantly lower and capacity correspondingly larger than that of the conventional B1-250 packing.

NOMENCLATURE

A_i	cell area, m^2
A_t	total column cross sectional area, m^2
C_v	coefficient of local velocity variation, -
C_m	coefficient of cluster velocity variation, -
F-factor	$(=u_{Gs}\,\rho G^{0.5})$ gas load factor, $(m/s)(kg/m^3)^{0.5}$ or $Pa^{0.5}$
MI	maldistribution index, -
N	total number of cells, -
$\overline{u}$	mean velocity, m/s
u_{Gs}	superficial gas velocity, m/s
u_i	local (cell *i*) velocity, m/s
u_j	local (cell *j*) velocity, m/s
$\overline{u}_i$	local mean (cluster) velocity, m/s

GREEK SYMBOLS

δ_{ij}	operator in equation (4)
ρ_G	gas (vapor) density, kg/m^3

ACKNOWLEDGEMENT

The authors are grateful to J. Montz GmbH for providing the packings and the distributor and for permission to publish the data.

This paper was presented at the AIChE Spring Meeting, Atlanta, GA, April 10–14, 2005.

REFERENCES

Billingham, J.F., Lockett, M.J., 1999, Development of a new generation of structured packings for distillation, Trans. IChemE (Part A) *Chem. Eng. Res. Des.* 77: 583–.

Killat, G.R., Rey, T.D., 1996, Properly Assess Maldistribution in Packed Towers, *Chem. Eng. Progress* 92(5): 69–.

Kister, H., 1992, *Distllation Design* (McGraw-Hill, New York, USA).

Moore, F., Rukovena, F., 1987, Liquid and gas distribution in commercial packed towers, *Chemical Plants and Processing* No. 8: 11–15.

Olujic, Z., de Graauw, J., 1989, Appearance of maldistributioin in distillation columns equipped with high performance packings, *Chem. Biochem. Eng. Q.* 3: 181–196.

Olujic, Z., de Graauw, J., 1990, Experimental studies on the interaction between the initial liquid distribution and the performance of structured packings, *Separation Science and Technology* 25: 1723–1735.

Olujic, Z., Stoter, C.F., de Graauw, J., 1992, Measurement of large scale gas and liquid maldistribution in structured packings, In Distillation and Absorption '92, IChemE Symp. Series No. 128: B-151–157.

Olujic, Z., Stoter, C.F., de Graauw, J., 1992, Performance evaluation of structured packings: Large- versus small scale, Preprints of the First Separations Division Topical Conference on Separation Technologies: New Developments and Opportunities, American Institute of Chemical Engineers, New York, pp. 201–208.

Olujic, Z., Jansen, H., Kaibel, B., Rietfort, T., Zich, E., 2001, Stretching the capacity of structured packings, *Ind. Eng. Chem. Res*. 40: 6172–6180.

Olujic, Z., Seibert, A.F., Kaibel, B., Jansen, H., Rietfort, T., Zich, E., 2003, Performance Characteristics of a New High Capacity Packing, *Chemical Engineering and Processing* 42: 55–60.

Pilling, M., Spiegel, L., 2001, Design Characteristics and Test Validation of High Performance Structured Packing, Separations Technology Topical Conference, AIChE Annual Meeting, November 4–9, Volume 1, pp. 64–69.

Potthoff, R., Stichlmair, J., 1991, Maldistribution in Packungskolonnen, *Chem.-Ing.- Techn*. 63: 72–.

Potthoff, R., 1992, Maldistribution in Füllkörperkolonnen, Fortschriftberichte VDI, Reihe 3: Verfahrenstechnik, Nr. 294 (VDI Verlag, Düsseldorf).

Stichlmair, J.G., Fair, J. R., 1998, *Distillation – Principles and Practice* (Willey-VCH, New York, USA).

Stoter, C.F., 1993, Modelling of Maldistribution in Structured Packings: from detail to column design, Thesis (Delft University of Technology, Delft).